

# We are IntechOpen, the world's leading publisher of Open Access books Built by scientists, for scientists

## 4,800

Open access books available

## 122,000

International authors and editors

## 135M

Downloads

Our authors are among the

## 154

Countries delivered to

## TOP 1%

most cited scientists

## 12.2%

Contributors from top 500 universities

**WEB OF SCIENCE™**Selection of our books indexed in the Book Citation Index  
in Web of Science™ Core Collection (BKCI)

Interested in publishing with us?  
Contact [book.department@intechopen.com](mailto:book.department@intechopen.com)

Numbers displayed above are based on latest data collected.

For more information visit [www.intechopen.com](http://www.intechopen.com)

# Synthesis, Characterization, Applications, and Toxicity of Lead Oxide Nanoparticles

*Amra Bratovic*

## Abstract

Over the past few years, the interest of material scientists for metal and metal oxide nanoparticles (NPs) is increasing dramatically because of their unique physicochemical characteristics such as catalytic activity and optical, electronic, antibacterial, and magnetic properties which depend on their size, shape, and chemical surroundings. Recently, several new routes of synthesis of lead monoxide (PbO) nanoparticles have been used, such as chemical synthesis, calcination, sol-gel pyrolysis, anodic oxidation, solvothermal method, thermal decomposition, chemical deposition, laser ablation, and green methods. Essentially, for the structural characterization of lead oxide nanoparticles, several spectroscopic, microscopic, and thermogravimetric methods of analysis are used. Lead oxide has been widely utilized in batteries, gas sensors, pigments, ceramics, and glass industry. Furthermore, lead oxide nanoparticles are graded as toxic and dangerous for the human health and environment. Therefore, there is an urgent need to develop new approaches and standardized test procedures to study the potential hazardous effect of nanoparticles on the human health and environment. The aim of this chapter is to provide an overview of the recent trends in synthesis of lead oxide nanoparticles, their characterization, possible applications, and toxicity.

**Keywords:** lead oxide nanoparticles, synthesis, characterization, applications, toxicity

## 1. Introduction

Today nanotechnology has become a top research field in the world. Nanotechnology is an interdisciplinary study which allows us to develop materials with new, interesting, and useful properties [1]. Nobel laureate Richard P. Feynman gave a lecture in 1959 at the annual American Physical Society meeting under title “There’s plenty of room at the bottom,” where he considered the possibility of direct manipulation of individual atoms as a more powerful form of synthetic chemistry than those used at that time [2]. Nanotechnology produced materials of various types at nanoscale level. Nanoparticles (NPs) are a large class of materials that include particulate substances having one dimension less than 100 nm at least [3]. Nanoparticles possess different properties and behave differently to the classical, larger building blocks of substances.

The world of nanotechnology is not new to mankind. The history of noble metal colloids can be traced back to ancient times. Cosmetic uses of lead-based chemistry were initiated in ancient Egypt about 4000 years ago [4].

**Figure 1** illustrates an increase in the number of published papers on ScienceDirect by searching the keyword “PbO nanoparticles” on November 28, 2019, indicating that researchers’ interest toward PbO nanoparticles continually increases since 2010.

Over the past few years, the interest of material scientists for metal nanoparticles has been booming because of its unique physicochemical characteristics such as a high specific surface area and a high fraction of surface atoms. The special properties of metal and metal oxide nanoparticles such as catalytic activity and optical, electronic, antibacterial, and magnetic properties [5–8] depend on their size, shape, and chemical surroundings [9] which can be designed by controlling the dimensions of these building blocks and their assembly via physical, chemical, or biological methods [10]. In particular, lead oxide electronic properties, i.e., bandgap and hence color, depend largely on the lead to oxygen ratios and crystal structures of various polymorphs.

Lead has a lot of oxide forms including PbO, PbO<sub>2</sub> ( $\alpha$ ,  $\beta$ , and amorphous), Pb<sub>2</sub>O<sub>3</sub>, and Pb<sub>3</sub>O<sub>4</sub>. Among them, lead monoxide (PbO) has been studied the most. Lead oxide is known as an important industrial material, which has been widely utilized in batteries [11], gas sensors [12], pigments and paints [13], ceramics [14], and glass industry [15] and as a catalyst in synthetic organic chemistry [16].

Different morphologies of lead oxide nanoparticles can play crucial roles in their properties. Lead oxide may appear in a various forms including nanoplates, nanostars and nanodendrites [17], nanorods [18], nanopowders [19], and nanosheets and nanotubes [20]. The color of tetragonal crystalline structure is red with  $\alpha$ -PbO form known as litharge and a bandgap of 1.9–2.2 eV, which has shown to be stable at room temperature, while orthorhombic crystalline structure is yellow with  $\beta$ -PbO form known as massicot and a bandgap of 2.7 eV, which seems to be stable at high temperatures, above 488°C [21]. The conversion phase of  $\alpha$ -PbO to  $\beta$ -PbO occurs at approximately 490°C. PbO yellow nanostructure possesses photoconductive properties.  $\alpha$ -PbO and  $\beta$ -PbO adopt similar open-packed rock salt-like structures which arise from the stereochemically active lone pair of Pb<sup>2+</sup> but with different orientations and distortions of PbO<sub>4</sub> pyramid units (**Figure 2**).

Pb atoms are shown as blue spheres and O atoms in red. The distances of adjacent Pb layers are drawn with lines for contrast [22].

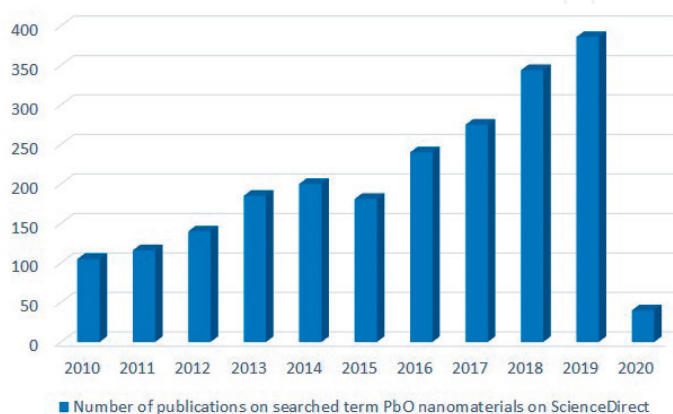


**Figure 1.**

*The results of published papers on ScienceDirect by searching the keyword “PbO nanoparticles.”*

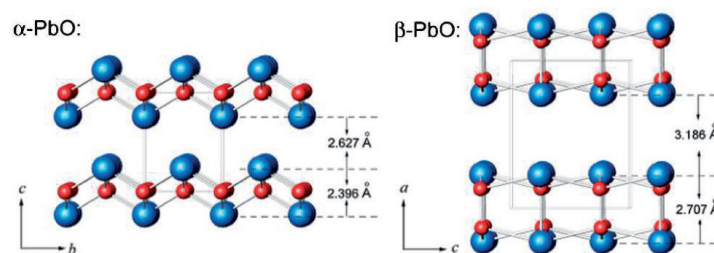


**Figure 2.**  
Crystal structures of  $\alpha$ -PbO and  $\beta$ -PbO.

## 2. Synthesis

In recent years, the synthesis of nanomaterials is an important topic of research in modern material science. For several years, scientists have constantly explored different synthetic methods to synthesize nanoparticles. Lead nanoparticles may be synthesized by three different methods, namely, physical, chemical, and green (biological) methods. Recently, several new routes of synthesis of PbO nanostructures have been used, such as chemical synthesis [23], calcination [24], sol-gel pyrolysis [25, 26], anodic oxidation [27], solvothermal method [16, 28, 29], thermal decomposition [30–32], chemical deposition [33], microwave irradiation technique [34], and green method [35].

Solvothermal synthesis is generally directed to crystal synthesis or crystal growth under high-temperature and high-pressure solvent conditions from substances which are insoluble in normal customary temperature and pressure in an autoclave.

Size-controlled preparation of semiconducting nanostructures is a major challenge in nanoscience and nanotechnology because their essential physicochemical properties and applications are forcefully related to the size-dependent quantum size effect. There has been a great attention of interest in developing various techniques for controlling the nanostructure sizes and shapes. Several studies have shown that in the course of the synthesis, a variety of factors including temperature, concentrations, the interplay between the metal ion precursors and the reducing agent, and adsorption kinetics are strongly influenced on the sizes, shapes, stability, and physicochemical properties of the nanostructures [36, 37].

Mathew and Krishnamurthy [38] in their study in 2018 have shown that the average size of the nanoparticles during chemical synthesis is higher than that during biological synthesis. The size of nanoparticles was found to be 1000 nm, whereas during biological synthesis the particle size was found to be 100–200 nm and above through dynamic light scattering. Using Debye-Scherrer equation, the particle size obtained through chemical synthesis was found to be 180 nm, whereas it was around 78 nm during biological synthesis.

The shape variation of the nanoparticles is important for several applications: oral delivery of therapeutic drugs and diagnostic materials, creation of the anti-bacterial coatings, and nanotoxicological research. Actually, the size, shape, and surface chemistry of nanoparticles can greatly impact cellular uptake and efficacy of the treatment. The results of the research carried out by Banerjee et al. [39] have shown that spherical nanoparticles in the co-culture have lower cellular uptake compared to rod-shaped nanoparticles regardless of the presence of active targeting moieties. Transport of spherical nanoparticles across the intestinal co-culture was also significantly lower than that of nanorods. This result indicates that nanoparticle-mediated oral drug delivery can be improved using rod-shaped nanoparticles instead of spherical shape.

The laser ablation in water gives the unique ability to produce the colloids (stable water suspensions) of spherical nanoparticles of pure metals and metal oxides. Shur et al. demonstrated the formation of the nonspherical particles at hot water treatment at a temperature above 70°C during laser ablation [40].

Method of synthesis	Source and conditions	Temperature/ time (°C)	Particle size (nm)	Reference
Chemical reactions	$\text{Pb}(\text{C}_2\text{H}_3\text{O}_3)_{2,3} \times \text{H}_2\text{O}$ + 19 M NaOH	90°C	TEM/SEM = 99 XRD = 60	[23]
Calcination	Lead citrate $\text{Pb}(\text{C}_6\text{H}_6\text{O}_7) \times \text{H}_2\text{O}$ Under $\text{N}_2$ and air	370°C, 20 min	$\text{N}_2$ : 50–60 Air: 100–200	[24]
Thermal decomposition	Lead stearate in octanol	80°C, 2–12 h	60–100 nm	[41]
	Lead hydroxycarbonate Urea and lead nitrate Under microwave	In vacuum at 90°C, 2 h Calcined at 400–600°C, 2 h	$\alpha$ -PbO = 30 $\beta$ -PbO = 38	[34]
	Lead oxalate ( $\text{PbC}_2\text{O}_4$ )	Precursor: 60°C, 7 h Calcined at 425°C, 3 h	20–30	[42]
Laser ablation	Lead plate that has 99.99% purity	Nd:YAG laser with laser energy of 400 mJ/pulse, with 1064 nm wavelength, 9 ns		[43]
	Pb of 99.99% purity		2D NPs and 3D NPs Micron and submicron diameter	[40]
Sol-gel	Lead nitrate Gelatin	60°C, 30 min 90°C Calcined at: 500–600°C under air, 2 h	TEM = 45	[44]
	Lead acetate (2.5 wt%) Polyvinyl alcohol (8 wt%) $\text{H}_2\text{O}/\text{EtOH}$ (40/60V/V)	80°C Calcined at 500°C, 5 h	18–43	[26]
Green/biosynthesis	$\text{Pb}(\text{NO}_3)_2$ Gelatin	90°C, 2 h Calcined at 450–600°C, 90 min	10–20	[45]
	Lead acetate, <i>Papaver somniferum</i>	60°C, 2 h Calcined at 500°C, 2 h	23 ± 11	[46]
	Lead nitrate Extract <i>cyminum</i>	Microwave 700 W 5 min	40–150 87 XRD = 35.8– 45.41	[35]

**Table 1.**  
An overview of the methods of synthesis and the main properties of Pb-NPs.



**Table 1** shows an overview of the methods of synthesis and the main properties of Pb-NPs.

It is noticeable from **Table 1** that the particle size decreases starting from chemical synthesis to sol-gel and green synthesis. It is possible to note that in the nitrogen atmosphere, the particle size is smaller (50–60 nm) than that done in air (100–200 nm). By changing the calcination temperature, it is possible to tune the ratio  $\alpha$ -PbO and  $\beta$ -PbO and consequently change the final properties of synthesized material. By using microwave instead of heating, it is possible significantly to reduce the reaction time and obtain the final material with different properties.

### 2.1 Chemical synthesis of lead oxide nanoparticles

Alagar et al. [23] have synthesized lead oxide (PbO) semiconductor nanoparticles by chemical synthesis. During this synthesis, they prepared 1 M aqueous solution of  $\text{Pb}(\text{C}_2\text{H}_3\text{O}_2)_{2.3} \text{H}_2\text{O}$  in deionized water and heated up to 90°C. They mixed this solution with an aqueous solution of 19 M NaOH and stirred vigorously. Immediately after mixing the two solutions, the cloudy solution is observed and then turned peach and finally deep orange red. At this moment, the reaction was stopped, and the formation of precipitate was evident. The supernatant was decanted, filtered on a Buchner funnel, washed with deionized water repeatedly, and dried overnight in a drying oven at 90°C. The sample was removed and lightly crushed in a mortar and pestle.

### 2.2 Calcination

Li et al. [24] have prepared nanostructural lead oxide by decomposition of lead citrate in inert (nitrogen) and in the air. The lead citrate [ $\text{Pb}(\text{C}_6\text{H}_6\text{O}_7) \cdot \text{H}_2\text{O}$ ], a precursor, was synthesized through leaching of spent lead-acid battery paste in citric acid system. In this citric acid leaching system,  $\text{C}_6\text{H}_8\text{O}_7 \cdot \text{H}_2\text{O}$  was used to supply the citric acid aqueous solution with distilled water for the balance of pH and for leaching and crystallization. The citrate particle was in the shape of sheets with the length of 10–20  $\mu\text{m}$ , width of 2–10  $\mu\text{m}$ , and thickness of 0.5  $\mu\text{m}$ .

The major decomposition products were orthorhombic phase  $\beta$ -PbO, metallic Pb, and elemental C, when the calcination was carried out in nitrogen gas. The ratio of  $\beta$ -PbO to Pb increased with the increasing temperature. The size range of the particle was 50–60 nm with a spherical shape. Lead citrate could be calcined completely within 20 min at 370°C in air conditions. The particle size obtained was in range of 100–200 nm. It was found to compose mainly of  $\beta$ -PbO with a small part of  $\alpha$ -PbO and Pb.

### 2.3 Synthesis by sol-gel method

In 2014 Yousefi and co-workers [44] have synthesized in a gelatin medium single-crystal, lead oxide nanoparticles (PbO-NPs) via the sol-gel method. In order to terminate the growth of the PbO-NPs and stabilize them, the long-chain gelatin compounds were utilized. The calcination of the gel obtained was done at 500, 550, and 600°C for 1 h. Miri et al. [45] have synthesized PbO-NPs through the utilization of gelatin as a green stabilizer.

### 2.4 Synthesis by thermal decomposition

The thermal decomposition of lead stearate in octanol was used by Akimov and co-workers [41] for the synthesis of lead nanoparticles. They showed that

by modifying the concentration of lead stearate in octanol and changing the thermolysis, time is possible to control the lead particle size. An organic coat composed of decomposition products of lead stearate prevents the particles from oxidation in air and favors their dissolution in organic solvents. Li et al. [34] have prepared PbO-NPs by thermal decomposition of lead hydroxycarbonate synthesized under microwave irradiation. Urea and lead nitrate were used as starting materials.

## 2.5 Green synthesis

Fundamentally, the main advantage of green method for the synthesis of nanoparticles is easy, efficient, and eco-friendly [38] in comparison to chemical-mediated or microwave-mediated green synthesis. The chemical synthesis involves toxic solvents, high pressure and energy, and high-temperature conversion, whereas microbe-involved synthesis is not feasible industrially due to its lab maintenance. Green biologically based methods which are safe, inexpensive, and an environment-friendly alternative usually imply the use of microorganisms and plants to synthesize nanoparticles [38, 47].

Nanoparticles can be synthesized from a wide variety of biological entities such as actinomycetes, algae, bacteria, fungus, plants, viruses, and yeast [48].

Gandhi et al. [35] have synthesized lead nanoparticles using the extract of *Cuminum cyminum* seed powder extract. The synthesized nanoparticles showed efficient antimicrobial activities against bacteria and pathogenic fungi. Similarly, the synthesized nanoparticles showed efficient anti-algal activity against spirulina culture.

## 3. Methods of characterization

For the structural characterization of lead oxide nanoparticles, several techniques are used including UV-visible spectrophotometry, FTIR spectroscopy, X-ray diffraction (XRD), energy-dispersive X-ray spectroscopy (EDX), scanning electron microscopy (SEM), thermogravimetric analysis (TGA), and thermogravimetric-differential thermal analysis (TG-DTA).

### 3.1 UV-visible studies

The optical properties of the PbO-NPs usually are studied by using a UV-visible (UV-vis) spectrophotometer. Many scientific papers indicate the presence of the absorption peaks in the visible region on the UV-vis absorption spectra of the PbO-NPs, which are attributed to the bandgap of the PbO-NPs with an orthorhombic phase [44]. The energy bandgap value of the prepared sample is 3.82 eV estimated using Tauc relation [23].

In the study of Miri et al. [45], the electronic spectra of the synthesized PbO-NPs have displayed a wide peak in 250–260 nm at the calcination temperatures of 450, 500, 550, and 600°C. They have discovered that by increasing the temperature from 450 to 600°C, the wavelength is repositioned from 252 to 260 nm, and the alpha form of PbO converts to beta.

The particle size of synthesized nanoparticles may be determined through the bandgap of electron spectrum by using the Tauc equation:

$$(\alpha h\nu) = A (h\nu - E_g)^n \quad (1)$$

where  $A$  is the absorption coefficient,  $h\nu$  is the photon energy, and  $E_g$  is the bandgap energy.

They have calculated values of bandgap energy for the synthesized PbO-NPs which were 4.38, 4.39, 4.30, and 4.02 eV at the calcination temperatures of 450, 500, 550, and 600°C, respectively. It is revealed that increasing the bandgap energy results in a smaller particle size. The calculated values of bandgap energy are much larger than the ordinary lead oxide bandgap indicating that the synthesized powder is in nanoscale and its alpha form is smaller than the beta. The bandgap energy of  $\alpha$ -PbO and  $\beta$ -PbO is 1.92 and 2.7 eV.

### 3.2 Fourier transform infrared (FTIR)

The chemical bonding of lead oxide NPs may be investigated by FTIR. According to Alagar et al. [23], two very sharp peaks at 466.74 and 557.39  $\text{cm}^{-1}$  on the FTIR spectra indicate the presence of lead and oxide.

FTIR spectrum for lead oxide nanoparticles synthesized by laser ablation of lead target immersed in deionized water by using pulsed Nd:YAG laser with laser energy of 400 mJ/pulse and different laser pulses has shown different transmission peaks [43]. The appearance of the transmission peak at 460  $\text{cm}^{-1}$  indicates the presence of (PbO) stretching vibration mode; the peaks located at (763.84, 1057.03)  $\text{cm}^{-1}$  and the peaks at (3877.05, 3742.03)  $\text{cm}^{-1}$  are corresponding to the bonding of (O—H) and harmonics of H—OH stretching bonding modes of water, while the infrared peaks located at (2856.67, 2918.40, 1743.1) and 1658.84  $\text{cm}^{-1}$  are related to the (C=O) stretching vibration modes that refer to little contribution of CO<sub>2</sub> dissolution from air contain.

The broad peak around 3400  $\text{cm}^{-1}$  corresponds to (O—H) stretching vibrations originating from small amount of ethanol used for washing the samples. A sharp peak at 1705  $\text{cm}^{-1}$  is assigned to vibrations of the carbonyl group (C=O), while another peak at 1395  $\text{cm}^{-1}$  is recognized as stretching vibration of carboxyl group (C—O). Metal-oxygen (M—O) stretching vibrations were identified by the peak presence in the region 300–900  $\text{cm}^{-1}$ .

### 3.3 X-ray diffraction (XRD)

X-ray powder diffraction (XRD) is a rapid analytical technique primarily used for phase identification of a crystalline material and can provide information on unit cell dimensions. The average grain size of lead oxide nanoparticles synthesized by chemical synthesis was determined using *Debye-Scherrer equation*.

The *Debye-Scherrer* equation is [49]:

$$D_{hkl} = K\lambda / (B_{hkl} \cos\theta) \quad (2)$$

where,

$D_{hkl}$  is the crystallite size in the direction perpendicular to the lattice planes.

$hkl$  are the Miller indices of the planes.

$K$  is a numerical factor frequently referred to as the crystallite-shape factor.

$\lambda$  is the wavelength of the X-rays.

$B_{hkl}$  is the width (full-width at half-maximum) of the X-ray diffraction peak in radians.

$\theta$  is the Bragg angle.

Specific surface area is 10.52  $\text{m}^2/\text{g}$ , surface area of particle is 11,304  $\text{nm}^2$ , particle volume is 113,040  $\text{nm}^3$ , and density value is 9.5  $\text{g}/\text{cm}^3$  [23]. Since the



crystallinity index is  $\approx 1.65$ , the sample is polycrystalline. The particle size (obtained from either TEM or SEM) is 99 nm, whereas that calculated from XRD is 60 nm [23].

In the research carried out by Yousefi et al. [44], XRD patterns indicated a phase transformation from tetragonal to orthorhombic as the calcination temperature increased from 500 to 600°C for 1 h. These Pb-NPs were synthesized by sol-gel method, and the SEM and TEM images showed that the nanoparticles started to form at a temperature range of 550–600°C. In addition, the TEM results showed that the average particle size of the nanoparticles was  $\sim 45$  nm. It is possible to note that by changing the method of synthesis, i.e., from chemical to sol-gel method, the nanoparticle size decreases from 60 [23] to 45 nm [44] and even to around 10–20 nm [45].

In the research carried out by Nafees et al. [42], X-ray diffraction (XRD) patterns were recorded in the  $2\theta$  range of 20–75 using a step size of  $0.05^\circ\text{s}^{-1}$ .

XRD pattern of PbO is indexed as tetragonal; a very small peak present at 30.25 ( $2\theta$ ) shows the presence of orthorhombic phase. Long heating time required to decompose  $\text{PbC}_2\text{O}_4$  precursor results in the phase change and a corresponding appearance of the additional peak. Average crystallite sizes for PbO and PbS were found to be around 20–30 nm as calculated by *Debye-Scherrer equation*.

### 3.4 Energy-dispersive X-ray spectroscopy (EDX)

For the identification and quantification of elemental compositions in a very small amount of material (few cubic micrometers of the sample), energy-dispersive X-ray spectroscopy (EDX) is used. The method is based on the excitation of the atoms on the surface by the electron beam, emitting specific wavelengths of X-rays that are the characteristic of the atomic structure of the elements. An energy-dispersive detector (a solid-state device that discriminates among X-ray energies) can analyze these X-ray emissions. Appropriate elements are assigned, yielding the composition of the atoms on the specimen surface [50].

### 3.5 Scanning electron microscopy (SEM)

SEM technique based on electron scanning provides all available information about the nanoparticles at nanoscale level. This technique is useful not only to study the morphology of the nanomaterials but also the dispersion of nanoparticles in the bulk or matrix. In the research carried out by Nafees and co-workers [42], lead oxalates ( $\text{PbC}_2\text{O}_4$ ) were used as a precursor for the synthesis of nanocrystalline lead oxide (PbO) by thermal decomposition.

### 3.6 Thermogravimetric analysis (TGA) and thermogravimetric-differential thermal analysis (TG-DTA)

Generally, the thermal analysis of TGA-DTA of the sample serves to obtain the proper calcination temperature to reach the pure phase. A better understanding of oxidation temperature/resistance and thermal stability of PbO and PbS is crucial for realizing the potential applications these materials promise. Still, sufficient literature on these issues is not available. Thermal stability and various transitions/reactions occur in nanostructured PbO and PbS during heat treatment in air and inert atmosphere [42]. In the research carried out by Miri et al. [45], the thermal analysis of TGA-DTA of the synthesized sample was performed in the temperature interval of 20–1000°C in an atmospheric air. On the DTA curve, the dehydration and discharge of crystalline and absorbed water were attributed in the temperature

range of 80–235°C. In the same temperature range on the TGA curve, the first weight loss of 35% was observed. In the temperature interval of 235–460°C, the second weight loss of 16% was attributed to the decomposition of gelatin chemical bond. In the temperature interval of 460–480°C, the third weight loss of 7% was related to lead oxidation, and the last weight loss of 6% was associated with the final oxidation of lead. Their study has discovered that PbO-NPs were stable in a temperature range between 550 and 880°C, since no weight changes were observed. In the same study, for the PbO, DSC/TGA curves were recorded from room temperature to 1175°C in air with the ramp rate of 10°C min<sup>-1</sup>. They observed that a mass loss of almost 2% occurs up to 500°C. As observed from differential thermogravimetric (DTGA) curve, dehydration takes place first resulting in the removal of water of crystallization around 100°C, while a hump between 200 and 250°C corresponds to the endothermic nature of transition confirmed by DSC curve. The thermal decomposition from PbO<sub>2</sub> to PbO occurs in a number of steps from 290 to 650°C accompanied by endothermic mass losses in designated temperatures. In DSC curve at 880°C, a sharp endothermic peak was observed indicating on the melting of PbO without the involvement of any mass loss as supported by TGA and DTGA curves. Probably because of the partial evaporation of very small PbO nanoparticles, another endothermic mass loss was observed around 1100°C.

Excellent thermal stability of PbO nanoparticles in a range from room temperature to 1175°C was attributed since only 2.7% of mass loss was recorded.

## 4. Applications

Lead oxide is a semiconductor nanostructure that has important applications in storage batteries, pigments, ceramics, and glass industry.

### 4.1 Storage batteries

Lead oxide has wide industrial applications as a basic material of electrode (anode and cathode) active mass in lead-acid batteries.

The lead-acid battery market is divided into industrial, data centers, telecom, oil and gas, and others. The industrial segment includes construction, metal and mining, chemical and pharmaceutical, and food and beverage industries. Due to the growth of the IT sector, Asia Pacific is focusing on increasing the number of data centers installed across the countries. It is expected that the lead-acid batteries will be used as a backup power solution in the data centers owing to their functionality across a wide temperature range. According to projections, the global lead-acid battery market could reach USD 52.5 billion by 2024 from an estimated USD 41.6 billion in 2019, at a CAGR of 4.7% during the forecast period. The booming telecommunication sector and expanding data industry require a cost-effective battery storage solution to provide for backup power [51].

Low-cost manufacture, simplicity of design, reliability, and relative safety are some of the advantages of lead-acid battery comparing to other electrochemical systems. Relatively, good specific power has caused a widespread use of lead-acid batteries in starting, lightening, and ignition of engine purposes for vehicular applications. Because of the advantages of lead-acid batteries, there is a big interest to improve and develop lead oxide nanostructures to obtain more discharge capacity and more life cycle [52].

In formation process, lead oxide can be converted to spongy lead in anode and lead dioxide in cathode. Some advantages of lead-acid batteries include low-cost manufacture, simplicity of design, reliability, and relative safety when compared

to other electrochemical systems [26]. Lead oxide nanoparticles (PbO-NPs) have well-known applications in lead storage batteries. Every vehicle which has a lead-acid battery uses 5–10 kg of lead oxide in its production. This represents vast uses of lead oxide on a worldwide basis. Batteries designed for multiple charge–discharge cycles are *traction batteries*, and red lead ( $\text{Pb}_3\text{O}_4$ ) oxide is used for their production. Traction batteries are used to power all manners of electrical vehicles including fork-lift trucks, golf carts, milk floats, etc. For standby power applications in case of main supply failure in hospitals, computer installations, and telecom networks, *stationary batteries* are required. Again, red lead ( $\text{Pb}_3\text{O}_4$ ) oxide is common in these units.

#### 4.2 Sensors

Li et al. [34] have prepared PbO-NPs ( $\text{Pb}_3(\text{CO}_3)_2(\text{OH})_2$ ,  $\alpha$ -PbO, and  $\beta$ -PbO) by using microwave irradiation technique. The reaction time was only 17 min and was significantly shortened from 4 h of conventional water bath heating method. Hence, the use of microwave irradiation technique is a fast, convenient, mild, energy-efficient, and environment-friendly route to produce the lead nanoparticles. For the preparation of the Pb(II)-selective electrode, cellulose acetate-acetone method which is simple, economical, and highly efficient to form membrane was used.  $\alpha$ -PbO nanoparticle obtained by calcining  $\text{Pb}_3(\text{CO}_3)_2(\text{OH})_2$  at  $400^\circ\text{C}$  also was used. Experiment results indicate that this electrode exhibited a Nernstian response for  $\text{Pb}^{2+}$  ion in a linear range of  $2.5 \times 10^{-5} \text{ mol L}^{-1}$  to  $1.0 \times 10^{-1} \text{ mol L}^{-1}$ . High selectivity for some metal ions, especially for the interference ions, such as  $\text{Cu}^{2+}$ ,  $\text{Ag}^+$ , and  $\text{Hg}^{2+}$ , were obtained.

#### 4.3 Pigments

The major lead pigment is the red lead ( $\text{Pb}_3\text{O}_4$ ), which is used principally in ferrous metal protective paints, and litharge, a bright yellow form of lead monoxide, still finds applications in the production of yellow pigments. The colors that contain lead-based pigments seem to have interesting properties including rustproof, anti-bacterial, and anti-algae, which are extensively employed in shipbuilding, construction skeleton, and road construction [45].

#### 4.4 Glass

The clarity and density of leaded glass crystal can be enhanced by the presence of 24–28% of lead oxide. The presence of lead oxide in television tube may reduce harmful radiation. Lead oxide in the optical fibers enhances the refractive index.

Lead oxides are also used in special optical glasses, X-ray protection glasses, etc. A lead oxide in glazes and enamels enhances the thermal, color, and wear properties of such coatings.

#### 4.5 Stabilizers

Lead oxide as lead stabilizers in polyvinylchloride (PVC) processing is used. They improve the thermal stability of PVC, allowing high-temperature processing, and the electrical and UV resistance properties.

#### 4.6 Ceramics

Glassy materials that experience controlled crystallization, usually achieved by a heating process in the presence of nucleating agents, are named glass-ceramics.

Almeida et al. [53] have shown that lead oxide is an important glass modifier not only for affecting the chemical and mechanical stabilities of glasses but also for improving their thermal and optical properties. They have designed and controlled  $\beta$ -PbO and  $3\text{PbO}\cdot\text{H}_2\text{O}$  crystalline phases in a lead borate glass using femtosecond-direct laser writing (fs-DLW) followed by chemical etching at room temperature. They demonstrated that for the glass crystallization, the etching in aqueous KOH solution was responsible, whereas the grooves produced by fs-laser pulses enable the selective crystallization in a predetermined 2D pattern. By using this method, phase transformation at the micrometer scale can be controlled.

#### 4.7 Anticancer and antimicrobial drugs

Several researches indicate that lead oxide nanoparticles may act as significant anticancer and antimicrobial drugs. Miri et al. [45] have synthesized lead oxide nanoparticles through the utilization of gelatin as a stabilizer and studied its cytotoxic effects on Neuo2A cancer cell line. The results of this research indicated that concentrations of PbO-NP under  $30\ \mu\text{g}/\text{mL}$  have insignificant toxicity. Muhammad et al. [46] have synthesized lead oxide (PbO) and iron oxide ( $\text{Fe}_2\text{O}_3$ ) nanoparticles starting from *Papaver somniferum* L. *Papaver somniferum*, also known as opium poppy and as an important member of *Papaveraceae* family. Poppy plant is well recognized for its diverse pharmacological potentials. Poppy seeds have the analgesic potency and are used as source of oil. Both NPs also showed considerable total antioxidant potential, free radical scavenging potential, and reducing power. PbO showed more potent anticancer activity than  $\text{Fe}_2\text{O}_3$  NPs. The antibacterial property results show that the antibacterial activity of the lead oxide NPs was inversely proportional to the size of the nanoparticles in both Gram-negative and Gram-positive. It has been found that Gram-positive bacteria possess greater sensitivity to the lead oxide nanoparticles compared with Gram-negative bacteria [43].

### 5. Toxicity

Lead oxide nanoparticles are graded as toxic and dangerous for the humans and environment. Lead and its compounds are extremely poisonous. Lead is a heavy metal whose toxicity is based on its selective and practically irreversible retention in the nerve cells. In them, it affects the energy balance, the signal transmission, and the flow of sodium, potassium, and calcium ions. A lot of lead is used as tetraethyl lead compound as a petro-fuel additive. With the combustion of gasoline, the lead enters the atmosphere and reaches the respiratory chain or the drinkable water in a form of very fine particles. Some of the lead is absorbed by plants and animals, so it reintroduces food into the human body. The major target for lead toxicity is the nervous system. Poisoning by the lead happens after the consumption of food or water polluted with lead but also after unplanned ingestion of contaminated soil, dust, or lead-based paint [54].

Nanoscale lead dioxide particles ( $\text{nPbO}_2$ ) formed inside lead-bearing pipes or lead-containing faucets in drinking water distribution systems can release toxic lead ions, causing drinking water contamination. Ng et al. [55] used adult medaka fish (*Oryzias latipes*) as an in vivo model to investigate the bioavailability and toxicity of  $\text{nPbO}_2$  in an intact animal. Both types of  $\text{PbO}_2$  particles, nanoscale [ $\text{nPbO}_2$ ] and microscale bulk [ $\text{bPbO}_2$ ], were chemically stable in dechlorinated tap water with low water solubility. However, both  $\text{nPbO}_2$  and  $\text{bPbO}_2$  could be reductively dissolved into  $\text{Pb(II)}_{\text{aq}}$  in both the intestine (major uptake route) and gills of the fish,



thereby enhancing hepatic Pb accumulation. The Pb content was greater in the gills, liver, and brain with nanoscale than in the microscale bulk PbO<sub>2</sub> particles. This *in vivo* evidence implies the possibility of increased risk of exposure to Pb dissolution from PbO<sub>2</sub> particles in the digestive system via drinking water, which can enhance the bioavailability of Pb uptake and toxicity in humans.

Recent studies have indicated that even lower blood Pb toxicity causes several metabolic, neurological, and behavioral disorders, as well as may be associated with impairment in psychological progress, diminished skeletal growth, and disturbances in cardiovascular function [56]. Lead poisoning is one of the most common professional diseases in industry. De facto, in industrial plants, lead is introduced into the body by inhalation of polluted air, in which lead or its compounds are contained in the form of smoke, dust, or vapor. The quantity of lead absorbed and the degree of poisoning depend on the concentration of lead in the air, its physical or chemical state with respect to the suitability for absorption, and the time of exposure of a worker in the contaminated space. In many industrially advanced countries, toxicity limits are set for the workers handling various toxic and hazardous materials widely used in the manufacturing batteries. In general, a worker's maximum allowable lead inhalation during an 8-h working period is 0.15 mg/m<sup>3</sup>. The toxic effect of lead is based on its selective and practically irreversible retention in the nerve cells. Lead affects the energy balance, the signal transmission, and the flow of sodium, potassium, and calcium ions.

## 6. Conclusions

Nanotechnology is an emerging field in the current global market, and the use of nanoparticles has shown enormous applications in every industrial sector due to its unique properties. The number of published scientific papers clearly shows that interest in PbO-NPs has been increasing year by year over the last 10 years. The lead oxide nanoparticles are one of the most industrially used metal nanoparticles.

The global lead-acid battery market is projected to reach USD 52.5 billion by 2024 because the booming telecommunication sector and expanding data industry require a cost-effective battery storage solution to provide for backup power.

Different ways of synthesis of PbO nanoparticles were present through the chapter with emphasis on different final properties of synthesized material as well as disadvantages of chemical and physical route, including generation of toxic chemicals which cause damage to the environment as well as humans and advantages of green synthesis. Therefore, to overcome the disadvantages of chemical and physical methods, the material scientists have proposed the new "green" synthesis pathways of nanoparticles which are a simple, fast, economical, convenient, energy-efficient, and environment-friendly way to produce lead oxide nanoparticles with multifarious applications. This is possible by changing the method of synthesis (process parameters, precursor concentration, temperature, atmosphere, the way of heating) to tune the final properties of synthesized lead oxide nanoparticles (particle size, optical, mechanical, catalytic properties).

The advantage of laser ablation is underlined because in water it is possible to produce the colloids of spherical nanoparticles of pure metals and metal oxides which are important for the creation of the antibacterial coatings and nanotoxicological research. However, lead oxide nanoparticles are graded as toxic and dangerous for the human and environment, and therefore there is an urgent need to develop new approaches and standardized test procedures to study the potential hazardous effect of nanoparticles on human health and environment.



## **Conflict of interest**

The author declares that she has no conflict of interest.

IntechOpen

IntechOpen

## **Author details**

Amra Bratovic  
Faculty of Technology, Department of Physical Chemistry and Electrochemistry,  
University of Tuzla, Tuzla, Bosnia and Herzegovina

\*Address all correspondence to: [amra.bratovic@untz.ba](mailto:amra.bratovic@untz.ba)

## **IntechOpen**

---

© 2020 The Author(s). Licensee IntechOpen. This chapter is distributed under the terms of the Creative Commons Attribution License (<http://creativecommons.org/licenses/by/3.0>), which permits unrestricted use, distribution, and reproduction in any medium, provided the original work is properly cited. 

## References

- [1] Bratovcic A. Different applications of nanomaterials and their impact on the environment. *SSRG International Journal of Material Science and Engineering*. 2019;5:1-7
- [2] Feynman RP. There's plenty of room at the bottom. *Engineering and Science*. 1960;22:22-36
- [3] Laurent S, Forge D, Port M, Roch A, Robic C, Vander Elst L, et al. Magnetic iron oxide nanoparticles: Synthesis, stabilization, vectorization, physicochemical characterizations, and biological applications. *Chemical Reviews*. 2010;110:2574-2574. DOI: 10.1021/cr900197g
- [4] Singh P, Kumari K, Vishvakarma VK, Mehrotra GK, Chandra R, Kumar D, et al. Metal NPs (Au, Ag, and Cu): Synthesis, stabilization, and their role in green chemistry and drug delivery. In: Singh R, Kumar S, editors. *Green Technologies and Environmental Sustainability*. Cham: Springer; 2017. pp. 309-337. DOI: 10.1007/978-3-319-50,654-8\_14
- [5] De Gaetano F, Ambrosio L, Raucci MG, Marotta A, Catauro M. Sol-gel processing of drug delivery materials and release kinetics. *Journal of Materials Science: Materials in Medicine*. 2005;16(3):261-265. DOI: 10.1007/s10856-005-6688-x
- [6] Crabtree JH, Burchette RJ, Siddiqi RA, Huen IT, Hadnott LL, Fishman A. The efficacy of silver-ion implanted catheters in reducing peritoneal dialysis-related infections. *Peritoneal Dialysis International: Journal of the International Society for Peritoneal Dialysis*. 2003;23(4):368-374
- [7] Królikowska A, Kudelski A, Michota A, Bukowska J. SERS studies on the structure of thioglycolic acid monolayers on silver and gold. *Surface Science*. 2003;532-535:227-232. DOI: 10.1016/S0039-6028(03)00094-3
- [8] Zhao G, Stevens SEJ. Multiple parameters for the comprehensive evaluation of the susceptibility of *Escherichia coli* to the silver ion. *Biometals*. 1998;11(1):27-32. DOI: 10.1023/a:1009253223055
- [9] Theivasanthi T, Alagar M. X-ray diffraction studies of copper Nanopowder. *Archives of Physics Research*. 2010;1(2):112-117
- [10] Singh M, Manikandan S, Kumaraguru AK. Nanoparticles: A new technology with wide applications. *Research Journal of Nanoscience and Nanotechnology*. 2011;1(1):1-11. DOI: 10.3923/rjnn.2011.1.11
- [11] Sonmez M, Kumar R. Leaching of waste battery paste components. Part 1: Lead citrate synthesis from PbO and PbO<sub>2</sub>. *Hydrometallurgy*. 2009;95:53-60. DOI: 10.1016/j.hydromet.2008.04.012
- [12] Sljukić B, Banks CE, Crossley A, Compton RG. Lead(IV) oxide-graphite composite electrodes: Application to sensing of ammonia, nitrite and phenols. *Analytica Chimica Acta*. 2007;587:240-246
- [13] Senvaitiene J, Smirnova J, Beganskiene A, Kareiva A. XRD and FTIR characterisation of lead oxide-based pigments and glazes. *Acta Chimica Slovenica*. 2007;54:185-193
- [14] Jaffe B, Roth R, Marzullo S. Properties of piezoelectric ceramics in the solid-solution series lead titanate-lead zirconate-lead oxide: Tin oxide and lead titanate-lead hafnate. *Journal of Research of the National Bureau of Standards*. 1955;55(5):239-254
- [15] Dumbaugh WH, Lapp JC. Heavy-metal oxide glasses. *Journal of*

the American Ceramic Society. 1992;75(9):2315-2326. DOI: 10.1111/j.1151-2916.1992.tb05581.x

[16] Tayebee R, Maleki B, Sabeti M. A new simple method for the preparation of PbO nanoparticles and implementation of an efficient and reusable catalytic system for the synthesis of 1H-pyrazolo[1,2-b]phthalazine-5,10-diones. *Journal of the Iranian Chemical Society*. 2017;14(6):1179-1188. DOI: 10.1007/s13738-017-1068-2

[17] Chen KC, Wang CW, Lee YI, Liu HG. Nanoflakes and nanostars of  $\beta$ -PbO formed at the air/water interface. *Colloids and Surfaces A: Physicochemical and Engineering Aspects*. 2011;373(1-3):124-129. DOI: 10.1016/j.colsurfa.2010.10.035

[18] Ghasemi S, Mousavi MF, Shamsipur M, Karami H. Sonochemical-assisted synthesis of nano-structured lead dioxide. *Ultrasonics Sonochemistry*. 2008;15(4):448-455. DOI: 10.1016/j.ultsonch.2007.05.006

[19] Kashani-Motlagh MM, Karami Mahmoudabad M. Synthesis and characterization of lead oxide nanopowders by sol-gel method. *Journal of Sol-Gel Science and Technology*. 2011;59(1):106-110. DOI: 10.1007/s10971-011-2467-y

[20] Shi L, Xu Y, Li Q. Controlled growth of lead oxide nanosheets, scrolled nanotubes, and nanorods. *Crystal Growth Design*. 2008;8(10):3521-3525. DOI: 10.1021/cg700909v

[21] Schottmiller JC. Photoconductivity in tetragonal and orthorhombic lead monoxide layers. *Journal of Applied Physics*. 1966;37(9):3505-3510. DOI: 10.1063/1.1708890

[22] Wang Y, Lin X, Zhang H, Wen T, Huang F, Li G, et al. Selected-control hydrothermal growths of  $\alpha$ - and  $\beta$ -PbO

crystals and orientated pressure-induced phase transition. *CrystEngComm*. 2013;15:3513-3516. DOI: 10.1039/c2ce26162f

[23] Alagar M, Theivasanthi T, Kubera Raja A. Chemical synthesis of nano-sized particles of lead oxide and their characterization studies. *Journal of Applied Sciences*. 2012;12(4):398-401. DOI: 10.3923/jas.2012.398.401

[24] Li L, Zhu X, Yang D, Gao L, Liu J, Vasant Kumar R, et al. Preparation and characterization of nano-structured lead oxide from spent lead acid battery paste. *Journal of Hazardous Materials*. 2012;203-204:274-282

[25] Mahmoudabad MK, Kashani-Motlagh MM. Synthesis and characterization of PbO nanostructure and NiO doped with PbO through combustion of citrate/nitrate gel. *International Journal of the Physical Sciences*. 2011;6(24):5720-5725

[26] Karami H, Ghamooshi-Ramandi M. Synthesis of sub-micro and nanometer sized Lead oxide by sol-gel pyrolysis method and its application as cathode and anode of Lead-acid batteries. *International Journal of Electrochemical Science*. 2013;8:7553-7564

[27] Singh DP, Srivastava ON. Synthesis of micron-sized hexagonal and flowerlike nanostructures of lead oxide (PbO<sub>2</sub>) by anodic oxidation of lead. *Nano-Micro Letters*. 2011;3(4):223-227. DOI: 10.1007/BF03353676

[28] Gao P, Liu Y, Bu X, Hu M, Dai Y, Gao X, et al. Solvothermal synthesis of  $\alpha$ -PbO from lead dioxide and its electrochemical performance as a positive electrode material. *Journal of Power Sources*. 2013;242:299-304. DOI: 10.1016/j.jpowsour.2013.05.077

[29] Jia B, Gao L. Synthesis and characterization of single crystalline PbO nanorods via a facile hydrothermal

- method. *Materials Chemistry and Physics*. 2006;**100**(2-3):351-354. DOI: 10.1016/j.matchemphys.2006.01.012
- [30] Salavati-Niasari M, Mohandes F, Davar F. Preparation of PbO nano-crystals via decomposition of lead oxalate. *Polyhedron*. 2009;**28**(11):2263-2267. DOI: 10.1016/j.poly.2009.04.009
- [31] Behnoudnia F, Dehghani H. Synthesis and characterization of novel three-dimensional-cauliflower-like nanostructure of lead (II) oxalate and its thermal decomposition for preparation of PbO. *Inorganic Chemistry Communications*. 2012;**24**:32-39. DOI: 10.1016/j.inoche.2012.07.031
- [32] Cimen E, Gumus I, Arslan H. The role of intermolecular interactions in the assembly of zinc(II) and Lead(II) complexes containing carboxylate ligand and their conversion to metal oxides. *Journal of Molecular Structure*. 2018;**1166**:397-406. DOI: 10.1016/j.molstruc.2018.04.024
- [33] Mythili N, Arulmozhi K. Characterization studies on the chemically synthesized  $\alpha$  and  $\beta$  Phase PbO nanoparticles. *International Journal of Scientific and Engineering Research*. 2014;**5**(1):412-416
- [34] Li S, Yang W, Chen M, Gao J, Kang J, Qi Y. Preparation of PbO nanoparticles by microwave irradiation and their application to Pb(II)-selective electrode based on cellulose acetate. *Materials Chemistry and Physics*. 2005;**90**:262-269. DOI: 10.1016/j.matchemphys.2004.02.022
- [35] Gandhi N, Sirisha D, Asthana S. Microwave mediated green synthesis of lead (Pb) nanoparticles and its potential applications. *International Journal of Engineering Sciences and Research Technology*. 2018;**7**(1):623-644. DOI: 10.5281/zenodo.1161701
- [36] Alexandridis P. Gold nanoparticle synthesis, morphology control, and stabilization by functional polymers. *Chemical and Engineering Technology*. 2011;**34**(1):15-28. DOI: 10.1002/ceat.201000335
- [37] Wang L, Chen X, Zhan J, Chai Y, Yang C, Xu L, et al. Synthesis of gold nano and microplates in hexagonal liquid crystals. *The Journal of Physical Chemistry B*. 2005;**109**(8):3189-3194. DOI: 10.1021/jp0449152
- [38] Mathew BB, Krishnamurthy NB. Evaluation of lead oxide nanoparticles synthesized by chemical and biological methods. *Journal of Nanomedicine Research*. 2018;**7**(3):195-198. DOI: 10.15406/jnmr.2018.07.00187
- [39] Banerjee A, Qi J, Gogoi R, Wong J, Mitragotri S. Role of nanoparticle size, shape and surface chemistry in oral drug delivery. *Journal of Controlled Release*. 2016;**238**:176-185. DOI: 10.1016/j.jconrel.2016.07.051
- [40] Shur VY, Gunina EV, Esin AA, Shishkina EV, Kuznetsov DK, Linker EA, et al. Influence of hot water treatment during laser ablation in liquid on the shape of PbO nanoparticles. *Applied Surface Science*. 2019;**483**:835-839. DOI: 10.1016/j.apsusc.2019.03.303
- [41] Akimov DV, Andrienko OS, Egorov NB, Zherin II, Usov VF. Synthesis and properties of lead nanoparticles. *Russian Chemical Bulletin, International Edition*. 2012;**61**(2):225-229. DOI: 10.1007/s11172-012-0032-7
- [42] Nafees M, Ikram M, Ali S. Thermal stability of lead sulfide and lead oxide nano-crystalline materials. *Applied Nanoscience*. 2017;**7**:399-406. DOI: 10.1007/s13204-017-0578-7
- [43] Rashed HH, Fadhil FA, Hadi IH. Preparation and characterization of lead oxide nanoparticles by laser ablation as antibacterial agent. *Baghdad Science*



Journal. 2017;**14**(4):801-807. DOI:  
10.21123/bsj.2017.14.4.0801

[44] Yousefi R, Khorsand Zak A, Jamali-Sheini F, Ming Huang N, Jeffrey Basirun W, Sookhakian M. Synthesis and characterization of single crystal PbO nanoparticles in a gelatin medium. *Ceramics International Part A*. 2014;**40**(8):11699-11703. DOI: 10.1016/j.ceramint.2014.03.180

[45] Miri A, Sarani M, Hashemzadeh A, Mardani Z, Darroudi M. Biosynthesis and cytotoxic activity of lead oxide nanoparticles. *Green Chemistry Letters and Reviews*. 2018;**11**(4):567-572. DOI: 10.1080/17518253.2018.1547926

[46] Muhammad W, Khan MA, Nazir M, Siddiquah A, Mushtaq S, Hashmi SS, et al. *Papaver somniferum* L. mediated novel bioinspired lead oxide (PbO) and iron oxide (Fe<sub>2</sub>O<sub>3</sub>) nanoparticles: In-vitro biological applications, biocompatibility and their potential towards HepG2 cell line. *Materials Science and Engineering: C*. 2019;**103**:109740. DOI: 10.1016/j.msec.2019.109740

[47] Shah M, Fawcett D, Sharma S, Tripathy SK, Poinern GE. Green synthesis of metallic nanoparticles via biological entities. *Materials*. 2015;**8**:7278-7308. DOI: 10.3390/ma8115377

[48] Thakkar KN, Mhatre SS, Parikh RY. Biological synthesis of metallic nanoparticles. *Nanomedicine*. 2010;**6**(2):257-262. DOI: 10.1016/j.nano.2009.07.002

[49] Holzwarth U, Gibson N. The Scherrer equation versus the “Debye–Scherrer equation”. *Nature Nanotechnology*. 2011;**6**:534. DOI: 10.1038/nnano.2011.145

[50] Ebnesajjad S. Surface and material characterization techniques. In: *Surface Treatment of Materials for Adhesive Bonding*. 2nd ed. Oxford,

GB and Waltham, USA: Elsevier; 2014. pp. 39-75. DOI: 10.1016/B978-0-323-26,435-8.00004-6

[51] Lead Acid Battery Market. Available from: [https://www.marketsandmarkets.com/Market-Reports/lead-acid-battery-market-161,171,997.html?gclid=CjwKCAiAx\\_DwBRAfEiwA3vwZYiEesj31IcKlfbxHx\\_no4V7GbUiuckyKiINXcVrJ\\_eW6EUR5kM9RqhoCwLAQAvD\\_BwE](https://www.marketsandmarkets.com/Market-Reports/lead-acid-battery-market-161,171,997.html?gclid=CjwKCAiAx_DwBRAfEiwA3vwZYiEesj31IcKlfbxHx_no4V7GbUiuckyKiINXcVrJ_eW6EUR5kM9RqhoCwLAQAvD_BwE) [Accessed: 13 January 2020]

[52] Shah MA. Lead oxide (PbO) nanoparticles prepared by a new technique for biomedical applications. *International Journal of Biomedical Nanoscience and Nanotechnology*. 2010;**1**(1):3-9. DOI: 10.1504/IJBNN.2010.034121

[53] Almeida JMP, Almeida GFB, Hernandes AC, Mendonça CR. Architecture of lead oxide microcrystals in glass: A laser and etching based method. *CrystEngComm*. 2016;**31**:5959-5964. DOI: 10.1039/C6CE01255H

[54] Elbossaty WF. Toxicology, biological activity, synthesis, and anti-microbial effects of lead nanoparticles. *Journal of Medical Physics and Applied Sciences*. 2017;**2**(2:4):1-4. DOI: 10.21767/2574-285X.100011

[55] Ng DQ, Chu Y, Tan SW, Wang SL, Lin YP, Chu CH, et al. In vivo evidence of intestinal lead dissolution from lead dioxide (PbO<sub>2</sub>) nanoparticles and resulting bioaccumulation and toxicity in medaka fish. *Environmental Science Nano*. 2019;**6**(2):580-591. DOI: 10.1039/C8EN00893K

[56] Shamshad M, Soorambail K, Prakash V. Absorption, LD50 and effects of CoO, MgO and PbO nanoparticles on mice “*Mus musculus*”. *Journal of Environmental Science, Toxicology and Food Technology*. 2015;**9**(2):32-38. DOI: 10.9790/2402-09213238